Green synthesis of silver nanoparticles using calamondin (*Citrus microcarpa*) peel essential oil and evaluation of their biological activities

Lam Bach Bao Phuong[1], Le Pham Tan Quoc[1*]

[1]*Institute of Biotechnology and Food Technology, Industrial University of Ho Chi Minh City, Ho Chi Minh City 700000, Vietnam*

**Author to whom correspondence should be addressed:*
Le Pham Tan Quoc
Institute of Biotechnology and Food Technology
Industrial University of Ho Chi Minh City
Ho Chi Minh City 700000, Vietnam
Email: lephamtanquoc@iuh.edu.vn
ORCID ID: 0000-0002-2309-5423

Please cite this article as: Phuong.B.B.L., Quoc.T.P.L. Green synthesis of silver nanoparticles using calamondin (Citrus microcarpa) peel essential oil and evaluation of their biological activities. *Mongolian Journal of Chemistry*, **26**(54), 2025, xx-xx
https://doi.org/10.5564/mjc.v26i54.4249

Green synthesis of silver nanoparticles using calamondin (*Citrus microcarpa*) peel essential oil and evaluation of their biological activities

Lam Bach Bao Phuong[1]: https://orcid.org/0009-0004-4152-609X

Le Pham Tan Quoc[1]: https://orcid.org/0000-0002-2309-5423

[1]*Institute of Biotechnology and Food Technology, Industrial University of Ho Chi Minh City, Ho Chi Minh City 700000, Vietnam*

ABSTRACT

The exceptional biological qualities of silver nanoparticles (AgNPs), including their antibacterial, antioxidant, and anti-inflammatory capabilities, have garnered a lot of interest. The synthesis of AgNPs using plant-derived compounds is considered an environmentally friendly method, limiting the use of toxic chemicals. Among them, natural essential oils, rich in flavonoids and terpenoids, have shown effective roles as reducing agents and stabilizers. Calamondin (*Citrus microcarpa*) peel essential oil (CmEO), which is notable for its high limonene and flavonoid content, was chosen as the green synthesis agent in this study. AgNPs were created by reducing $AgNO_3$ with CmEO, and they were examined using UV-Vis, FTIR, DLS, and SEM. Dynamic light scattering (DLS) and SEM based on the analysis, it was observed that the AgNPs-CmEO possessed a spherical morphology with an average particle size of approximately 204.3 nm. The UV–Vis spectrum exhibited a characteristic surface plasmon resonance peak around 420 nm. In addition, both Gram-positive and Gram-negative bacteria were susceptible to the antibacterial activity of AgNPs-CmEO. However, the activity was still lower than that of gentamicin. The antioxidant activity was moderate, with IC_{50} of 617.37 µg/mL (DPPH) and 385.48 µg/mL (ABTS). Overall, CmEO is a potential bioreducing agent for AgNPs synthesis, opening up potential applications in food preservation and biomedicine while indicating the need for further process optimization to improve product performance and stability.

Keywords: antioxidant activity, antibacterial activity, essential oil, silver nanoparticles, green synthesis.

INTRODUCTION

To date, nanotechnology research has made great strides, allowing scientists to tailor the structure of silver particles at the nanoscale, thereby fine-tuning how they function in living systems and expanding their range of applications. Silver nanoparticles (AgNPs) have attracted considerable interest because of their remarkable biological activities, such as antibacterial, antioxidant, and anti-inflammatory activities [1]. The synthesis of silver nanoparticles using plant extracts represents a green and sustainable approach, offering an eco-friendly alternative to conventional chemical and physical methods, which helps to eliminate the need for hazardous chemicals and reduces negative impacts on the environment. Essential oils stand out as plant-based green reducers because they house plenty of active agents-flavonoids, terpenoids, and phenolic acids-that drive the particle-formation process [2]. When paired with silver ions, these oils can yield nanoparticles with enhanced potential as antimicrobial coatings, contributing to extended food shelf-life and improved safety. Yet, conventional lab recipes still rely on harsh add-ins, such as $NaBH_4$, citrate, or hydrazine, that harm both ecosystems and the people who handle them [3]. This has stimulated interest in greener, safer, and more sustainable alternatives, notably the use of natural reducing agents, among which plant extracts and particularly essential oils are emerging as promising options [4].

Essential oil of calamondin (*Citrus microcarpa*) is recognized for its diverse phytochemical composition, particularly its high content of limonene, flavonoids, and other antioxidant compounds [5]. These phytochemicals not only function as electron donors that convert silver ions (Ag^+) into elemental silver (Ag^0) but also function as stabilizers, preventing nanoparticle aggregation and thereby improving their stability and biological efficacy [6]. A notable aspect is that calamondin essential oil is extracted from agricultural by-products; therefore, the combination of nanotechnology and the use of agricultural waste not only yields high economic efficiency but also contributes to environmental protection. Compared to traditional chemical methods, the use of calamondin essential oil offers a greener and more cost-

effective solution, leveraging natural compounds to enhance the properties of silver nanoparticles [7].

Silver nanoparticles made using calamondin essential oil show promising usefulness in medicine, food storage, and cosmetics [8]. Our work highlights calamondin oil as a clean and eco-friendly reducing agent for nanoparticle synthesis. Leaning on the oils natural chemistry not only spares harmful reagents but also boosts the nanomaterials performance, supporting their broader application in sustainable nanotechnology in several industries.

EXPERIMENTAL

Plant extraction

Essential oil of calamondin (CmEO) is extracted from the peel of *Citrus microcarpa* collected in Dong Nai Province, Vietnam, using the steam distillation method. Based on GC–MS analysis, the predominant constituents of CmEO are 72.69% D-limonene, 22.53% α-Pinene, 2.27% γ-Terpinene, and 1.84% citral.

Bacterial strains

The study utilized four bacterial strains, comprised two Gram-positive strains-*Staphylococcus aureus* (ATCC 33591) and *Bacillus cereus* (ATCC 11778)-and two Gram-negative strains-*Escherichia coli* (ATCC 25922) and *Salmonella enteritidis* (ATCC 13076). The bacterial strains utilized in this research were supplied by the Institute of Biotechnology and Food Technology, Ho Chi Minh City University of Industry.

Chemicals

Among the substances utilized in the investigation were 2,2-diphenyl-1-picrylhydrazyl (DPPH, purity ≥97%, Sigma, USA), 2,2'-azinobis(3-ethylbenzothiazoline-6-sulfonic acid) (ABTS, ≥98%, Sigma, USA), silver nitrate ($AgNO_3$, China), and dimethyl sulfoxide (DMSO, purity ≥99.5%, China). In addition, the chemicals that meet analytical grade, along with the culture media and antibacterial testing such as nutrient broth, Mueller-Hinton agar (HiMedia, India), and other analytical grade chemicals were utilized in the study.

Experiment

Preparation of AgNPs with CmEO

The preparation method follows Maciel *et al.*, with minor tweaks. Oil was first diluted in acetone (1:100 v/v) for quick mixing [9]. We then made a 5 mM $AgNO_3$ solution and raised the pH to 8 with 2 M NaOH. Subsequently, the diluted essential oil in 5 milliliters was gradually introduced into 50 mL of $AgNO_3$ solution at 50 °C, with constant stirring at 600 rpm for 1 hour to facilitate nanoparticle formation. The mixture turned golden brown, a clear sign that AgNPs had formed. The finished particles were kept at 6°C for storage.

Characterization of AgNPs

According to Quidwai *et al.*, AgNPs morphology, size, and chemical composition were evaluated by using UV-Vis spectrophotometry (300-700 nm), dynamic light scattering (DLS), scanning electron microscopy (SEM), and Fourier-transform infrared spectroscopy (FTIR) [10].

Determination of antioxidant activity using DPPH assay

To determine antioxidant capability, its free radical scavenging ability was evaluated through the DPPH assay, adapted from Quoc and Phuong [11]. The AgNPs was dissolved in 96% ethanol to create solutions of different concentrations. For each sample, 2.7 mL of 0.1 mM DPPH was mixed with 0.3 mL of the test solution and stored for half an hour at room temperature in the dark. Next, using vitamin C as the standard, the absorbance was measured at 517 nm. The inhibition percentage and IC_{50}, the concentration at which 50% inhibition occurred, were computed. The antioxidant capacity was subsequently calculated using a formula comparing the sample and control absorbance values.

$$\%\mathrm{DPPH}_{\mathrm{RSC}} = \frac{\mathrm{A}_{\mathrm{control}} - \mathrm{A}_{\mathrm{sample}}}{\mathrm{A}_{\mathrm{control}}} \times 100$$

where $A_{control}$ denotes the absorbance of DPPH solution, while A_{sample} refers to the absorbance of AgNPs conjugated with DPPH solution.

Determination of antioxidant activity using ABTS assay

The antioxidant potential was evaluated following the method described by Le *et al.* [12]. The mixture of 7 mM $ABTS^+$ and 2.45 mM potassium persulfate

was combined in equal volumes (1:1, v/v) with distilled water and left to react for 16 hours at room temperature in the dark. After preparation, the solution was diluted appropriately to a 0.70 ± 0.02 absorbance at 734 nm. After mixing 0.1 mL of AgNPs solutions (various concentrations) with 3 mL of the ABTS solution, ethanol was added to produce a final volume of 5 mL. Absorption was recorded at 734 nm after a 6-minute period in darkness. The inhibition percentage, IC_{50}, and antioxidant capacity (AC) were calculated based on a defined equation.

$$\%\mathrm{ABTS}_{\mathrm{RSC}} = \frac{\mathrm{A}_{\mathrm{control}} - \mathrm{A}_{\mathrm{sample}}}{\mathrm{A}_{\mathrm{control}}} \times 100$$

where $A_{control}$ denotes is the absorbance value of the ABTS radical solution, while A_{sample} indicates the absorbance measured for the sample conjugated with ABTS solution.

Determination of antibacterial activity

Antibacterial efficacy was determined by a modified using paper disk diffusion method, referencing Sripahco ***et al.*** [13]. Standardized to 0.5 McFarland (about 1.5×10^8 CFU/mL), bacterial suspensions (0.1 mL) were evenly laid onto MHA agar plates. Five µL AgNPs loaded sterile six-mm paper discs. The positive and negative controls were gentamicin (10 µg/disc) and 5% DMSO, respectively and 5% DMSO were used as the positive and negative controls, respectively. The antibacterial effect was assessed by dertermining the inhibitory zones' diameter after a 24-hour static incubation period at 37°C.

Effects of AgNPs on S. aureus growth rate

S. aureus (ATCC 33591), a methicillin-resistant strain, was specifically selected to highlight the clinical relevance of using AgNPs-CmEO against antibiotic-resistant pathogens [14]. The effect of AgNPs on the growth rate of *S. aureus* was examined by incubating bacterial cultures with AgNPs at concentrations of 5 mM. Absorbance readings at 600 nm, taken over a 10-hour period (0-10 hours), provided a measure of bacterial density, thereby reflecting the growth kinetics. This approach, based on Ceylan and Doğru, enables the determination of AgNPs' inhibitory effect on *S. aureus* growth, potentially revealing concentration-dependent antibacterial activity [15].

Analysis method

The information was assessed using variance analysis (ANOVA) and mean comparison tests with Statistics 20 software. Statistical differences among samples were determined using Tukey's HSD test with a 95% accuracy level ($p < 0.05$). The data are presented as mean ± standard deviation.

RESULTS AND DISCUSSION

Nanoparticles synthesis

The transformation of silver nitrate ($AgNO_3$) into elemental silver occurred through the action of reducing compounds in the CmEO extract, leading to the generation of AgNPs. This transformation was often associated with a pronounced development of color within the reaction mixture, changing from colorless to yellow-brown (Fig. 1). During 60 min of continuous stirring, the mixture turned brown, indicating an increased concentration of nanoparticles. This noticeable color shift, which was ascribed to surface plasmon resonance excitation (SPR) in the nanoparticles and served as primary evidence for the successful formation of AgNPs [12]. Compared with other green synthesis approaches, such as the study of Le *et al.* [12] using *Mentha aquatica* extract that required up to 24 h of reaction time, the 60 min reaction time observed in this study demonstrates a markedly faster biosynthesis process, underscoring the efficiency of CmEO as both a bioreducing and agent that stabilizes in AgNPs production.

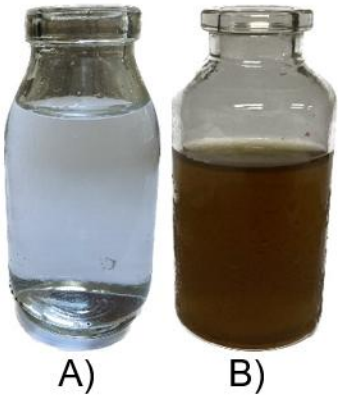

Fig.1. Color transformation observed during AgNPs-CmEO synthesis (A) – prior to nanoparticle formation; (B) – nanoparticle formation

Uv-Vis analysis

The UV–Vis spectrum of the AgNPs produced using CmEO exhibited a distinct 420 nm is the middle of the surface plasmon resonance (SPR) band (Fig. 2), typically associated with the SPR effect of silver nanoparticles [16]. This observation is in line with earlier reports on the biosynthesis of AgNPs using plant-derived compounds. The formation of AgNPs-CmEO was further as evidenced by the way that a light brown coloration in the reaction mixture, a feature commonly ascribed to the absorption and scattering of visible light by silver nanoparticles. The intensity and shade of this color are affected by the size, morphology, and dispersion of the AgNPs in the solution [17].

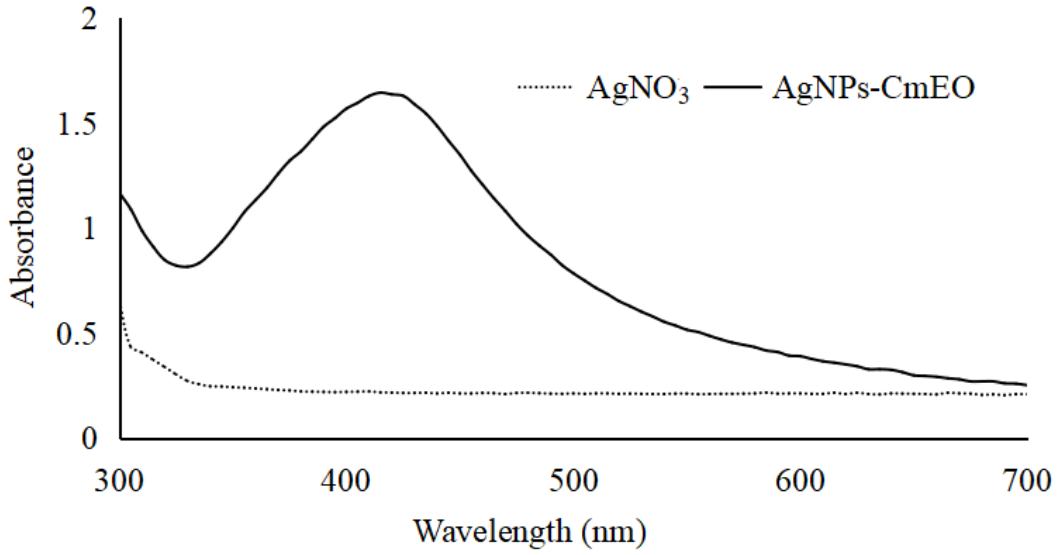

Fig.2. UV-Vis spectral analysis of AgNPs-CmEO

Compared to previous studies utilizing olive leaf extract during the formation of AgNPs, where the absorption a characteristic 449 nm was the observed absorption peak, the absorption peak of AgNPs synthesized from CmEO exhibits a shift to a shorter wavelength [15]. This shift is likely attributed to differences in the phytochemical composition of plant materials. In the CmEO, compounds such as limonene, flavonoids, and organic acids could be important in regulating the size of the nanoparticles and influencing their optical properties. This shift may reflect the development of silver nanoparticles with smaller dimensions or exhibit distinct interactions with the surface-stabilizing compounds present in the essential oil.

Fourier transform infrared (FTIR) spectroscopy

Silver ions (Ag^+) are reduced and silver nanoparticles (AgNPs-CmEO) are stabilized by the presence of important functional groups, according to the FTIR (Fourier Transform Infrared) spectra of AgNPs-CmEO (Fig. 3).

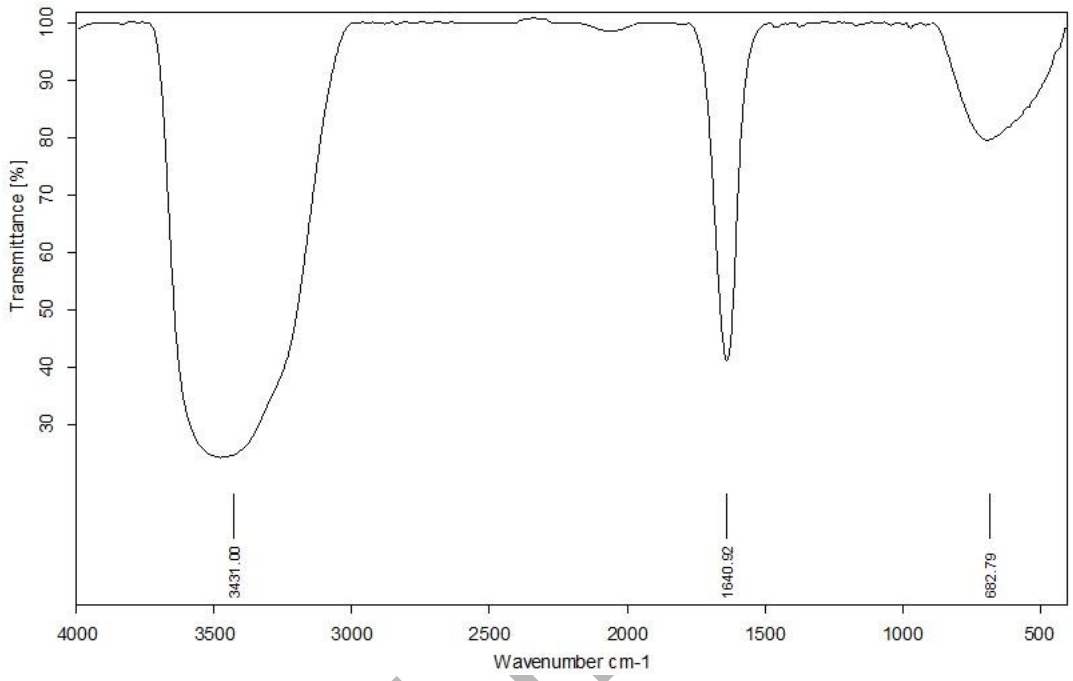

Fig.3. Fourier transform infrared (FTIR) spectra of AgNPs-CmEO

Specifically, when –OH group stretching vibrations are present, an absorption peak at about 3400 cm^{-1} is present, indicating the presence of compounds capable of forming hydrogen bonds, such as polyphenols or flavonoids [18]. The distinctive C=O stretching vibration of the carbonyl group, which is frequently present in compounds like aldehydes, ketones, or organic acids, is identified by the peak at about 1700 cm^{-1} [19].

Furthermore, the FTIR peak at approximately 1450 cm^{-1} is connected to the bending vibrations of the CH_2 group, while the peak around 1100 cm^{-1} relates to the stretching vibrations of the C-O bond, which is commonly present in terpenoid and ester compounds [20].

The detection of –OH and C=O functional groups confirms the role of phenolic and terpenoid compounds in CmEO when Ag^+ ions are reduces to Ag°. After the synthesis of AgNPs-CmEO, several peaks exhibited changes in intensity and position, indicating that these functional groupings are involved in stabilizing the silver nanoparticle surface. This implies that in addition to

serving as reducing agents, the organic compounds found in essential oils may also aid in the stabilization of the particles, preventing aggregation and regulating AgNPs size [21].

Dynamic light scattering (DLS) analysis

Based on dynamic light scattering (DLS) analysis, silver nanoparticles (AgNPs) synthesized from CmEO have a typical size of 204.3 nm and a polydispersity index (PDI) of 0.337, indicating a uniform size distribution (Fig. 4).

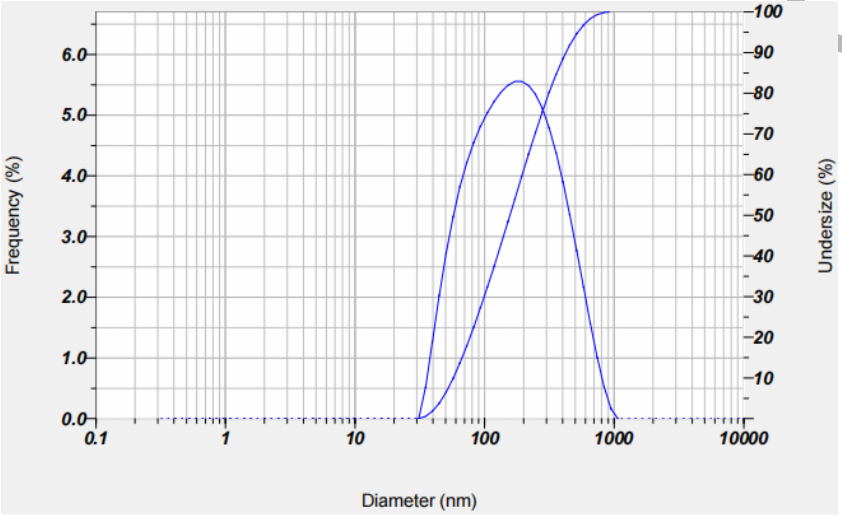

Fig.4. AgNPs-CmEO distribution as revealed by DLS measurements (DLS)

Although many studies have reported silver nanoparticles with average sizes typically below 100 nm. However, Kumar *et al.* [22] observed the AgNPs displayed an average size of 113.6 nm (distribution 34–400 nm). In this context, our results are comparable, as the particles still fall within the nanoscale range, thereby retaining characteristic properties such as high surface reactivity and localized surface plasmon resonance (LSPR). Variations in particle size may result from multiple factors, including the concentration and chemical composition of CmEO, together with synthesis parameters like reaction duration, temperature, and pH. The phytochemical constituents of CmEO, particularly limonene, flavonoids, and organic acids, are likely to influence the nucleation and growth of nanoparticles, ultimately determining their final dimensions [23]. The PDI value of 0.337 suggests a moderate degree of polydispersity, which indicates acceptable colloidal

stability [24]. While optimization of synthesis conditions is still required to achieve a more homogeneous particle system, AgNPs derived from CmEO nonetheless demonstrate potential for applications in antibacterial activity, catalysis, and biomedicine.

Scanning electron microscopy (SEM) analysis

The silver nanoparticles (AgNPs) made from CmEO primarily have a spherical morphology, which is a feature of biologically synthesized AgNPs-CmEO, according to Scanning Electron Microscopy (SEM) (Fig. 5). This observed morphology aligns with earlier reports on the biosynthesis of AgNPs-CmEO, wherein organic compounds derived from plant extracts or EO serve as reducing and stabilizing agents, facilitating the control of particle formation [25].

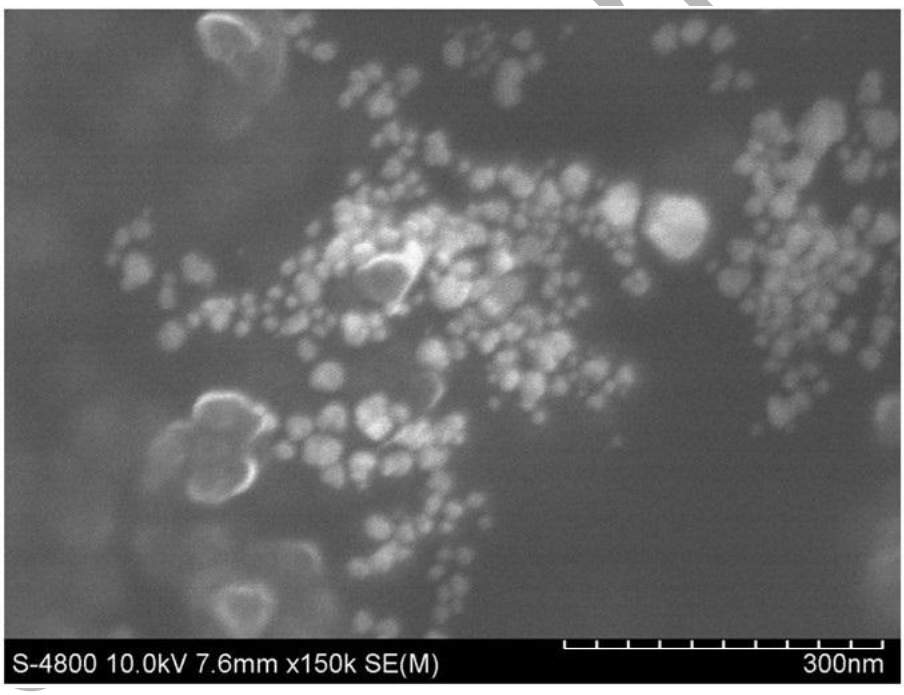

Fig.5. Scanning electron microscopy (SEM) images of AgNPs-CmEO

SEM observations revealed a tendency of some particles to aggregate, which may be attributed to the relatively high particle concentration of particles in the solution and the limited efficiency of stabilizing agents in preventing interparticle adhesion. This phenomenon is commonly encountered in studies synthesizing AgNPs-CmEO, particularly when employing biological methods,

as biomolecules do not always produce a uniform surface coating to mitigate aggregation [26].

In comparison with the DLS results, the particle size observed from the SEM images is consistent with the previously measured values, indicating coherence between the two analytical methods. The particle surface is relatively uniform, showing no signs of abnormal morphology or uncontrolled crystallization.

Determination of the antioxidant activity

The research results indicate that AgNPs synthesized using CmEO exhibit moderate antioxidant activity, with a value $IC_{50\text{-DPPH}}$ = 617.37 µg/mL and $IC_{50\text{-ABTS}}$ = 385.48 µg/mL (Table 1). Compared to vitamin C - a standard substance with strong antioxidant properties ($IC_{50\text{-DPPH}}$ = 3.47 µg/mL, $IC_{50\text{-ABTS}}$ = 7.38 µg/mL), the activity of silver nanoparticles is significantly lower. This is consistent with the general characteristics of nanomaterials, wherein the antioxidant efficacy depends on the free radical mechanism neutralization and the surface properties of the nanoparticles.

Table 1. DPPH and ABTS assay for antioxidant activity of AgNPs-CmEO

Test sample	$IC_{50\text{-DPPH}}$	$IC_{50\text{-ABTS}}$
Vitamin C (µg/mL)	$3.47^{A} \pm 0.27$	$7.38^{B} \pm 0.25$
AgNPs-CmEO (µg/mL)	$617.37^{B} \pm 4.38$	$385.48^{B} \pm 5.47$

Significant variations ($p \leq 0.05$) are indicated by different letters (A–B) between samples within a column.

When compared to previous studies, silver nanoparticles synthesized using calamondin essential oil exhibit superior antioxidant activity. For instance, AgNPs synthesized from *M. aquatica* showed much weaker activity (IC_{50}-DPPH = 1290 µg/mL, IC_{50}-ABTS = 1480 µg/mL) [12]. However, this efficacy is still significantly lower compared to silver nanoparticles synthesized using

Taraxacum officinale, with $IC_{50\text{-DPPH}}$ = 56.1 μg/mL and $IC_{50\text{-ABTS}}$ = 45.6 μg/mL [27].

The chemical composition of plant extracts is a key factor underlying such variations. In the case of CmEO, limonene is the dominant constituent, which is a hydrocarbon monoterpene with relatively weak radical-scavenging potential compared to phenolic-rich extracts [28]. Although flavonoids present in CmEO may contribute to some antioxidant capacity, their lower abundance limits the overall activity. Furthermore, the relatively larger particle size of AgNPs-CmEO (204.3 nm) may reduce the effective surface area available for interaction with free radicals. By contrast, extracts richer in phenolic compounds, such as those from *Taraxacum officinale* [27], can produce smaller nanoparticles with higher surface reactivity, thereby enhancing antioxidant performance [29].

The chemical structure of plant extracts may be the cause of the variation in activity since it influences the size, shape, and surface properties of nanoparticles, which in turn affects their antioxidant capacity.

Determination of the antibacterial activity of AgNPs

The experimental results indicate shows all four of the examined bacterial strains are susceptible to the antibacterial action of AgNPs (Table 2), with the inhibition zone diameter ranging from 13.55 mm to 19.57 mm. The highest efficacy was recorded against *S. enteritidis* (19.57 mm), followed by *B. cereus* (17.40 mm), *E. coli* (16.04 mm), and the lowest against *S. aureus* (13.55 mm). Compared to the antibiotic gentamicin, the CmEO exhibits significantly lower inhibitory efficacy ($p \leq 0.05$), indicating that the antibacterial capability of AgNPs-CmEO may depend on concentration and mechanisms of action that differ from those of synthetic antibiotics.

Table 2. Antibacterial zones of AgNPs-CmEO

Test strains	Diameter of the inhibitory zones of gentamicin (mm)	Diameter of the inhibitory zones of AgNPs (mm)

E. coli	$24.72^{Bb} \pm 0.55$	$16.04^{Ba} \pm 0.27$
S. enteritidis	$31.39^{Db} \pm 1.04$	$19.57^{Da} \pm 0.37$
S. aureus	$20.29^{Aa} \pm 0.45$	$13.55^{Ab} \pm 0.80$
B. cereus	$26.39^{Cb} \pm 0.62$	$17.40^{Ca} \pm 0.12$

Significant differences ($p < 0.05$) are shown by different letters. between samples or microorganisms within a row (a–b) or column (A–D), respectively.

When compared to previous studies, the CmEO exhibits significantly lower antibacterial activity against *S. aureus* (13.55 mm) than the chitosan-silver nanoparticle membrane combined with cinnamon essential oil by Lestari *et al.* (19.5 mm) [30]. Similarly, the study by Adame *et al.* utilizing a biofilm containing essential oil from *Litsea cubeba* also demonstrated higher antibacterial activity, with 18.59 mm against *S. aureus* and 17.32 mm against *E. coli*, whereas AgNPs-CmEO only achieved 16.04 mm against *E. coli* [31]. This disparity may result from the essential oil's chemical makeup and modes of action on bacteria, as well as from the addition of other substances (chitosan, pullulan/cassava starch) that strengthen antibacterial qualities.

The research results indicate that the silver nanoparticle system combined with calamondin essential oil (AgNPs-CmEO) exhibits moderate antibacterial activity compared to previous studies utilizing substrate materials such as chitosan or pullulan. This difference may be elucidated through the specific mechanisms of action inherent to the system: Silver nanoparticles (AgNPs) primarily exert their effects through the release of Ag^+ ions, which cause damage to the membrane of the cell and generate reactive oxygen species (ROS), while the CmEO, with its main components being limonene and β-pinene, primarily disrupts the lipid bilayer of bacterial membranes [32, 33]. However, the lack of support from the substrate material has limited the ability to control the release and uniform distribution of active compounds, resulting in lower efficacy compared to three-component systems (silver nanoparticles - essential oils - substrate material). This underscores the importance of designing the delivery system in optimizing antibacterial activity.

Effects of AgNPs on S. aureus growth rate

Based on the data from Fig. 6, it can be observed that at a concentration of 5 mM AgNPs-CmEO, there is a trend towards inhibiting *S. aureus* increase in comparison to the control group. Although the optical density continues to increase over time, particularly at the 5 mM concentration, this is evidenced by a significant difference in the time interval from 2 hours to 8 hours. This indicates that AgNPs-CmEO, regardless of concentration, exerts a partial inhibiting effect on bacterial growth. However, the continued increase in absorption suggests that AgNPs-CmEO does not completely inhibit the growth of *S. aureus*, but may only slow down this process or induce physiological changes in the bacteria.

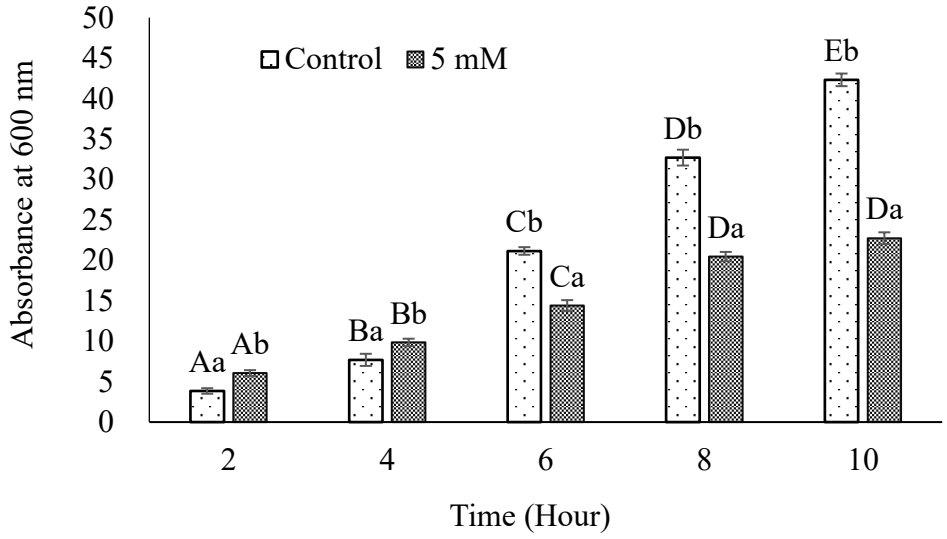

Fig.6. Time-dependent kinetic analysis of AgNPs-CmEO at two different concentrations against *S. Aureus*. Within each time period or category, distinct letters (a–b or A–E) denote significant differences ($p < 0.05$).

This result is consistent with the research carried out by Ceylan and Doğru when they looked into the biological activity of silver nanoparticles synthesized from *Olea europaea* L. leaves [15]. In their research, AgNPs-CmEO also demonstrated the capacity to prevent the growth of bacteria, although the level of inhibition may vary based on the level of concentration of AgNPs-CmEO and the type of bacteria employed. This further reinforces the evidence regarding the antibacterial properties of AgNPs-CmEO and the necessity for more in-depth studies to elucidate their mechanisms of action.

CONCLUSIONS

Calamondin (*Citrus microcarpa*) peel essential oil was used in this study as a stabilizing and reducing agent to successfully demonstrate the environmentally friendly synthesis of silver nanoparticles. The formation and stability of the biosynthesized AgNPs were confirmed by characterization using UV-Vis spectrophotometry, SEM, DLS, and FTIR. The AgNPs' notable free radical scavenging activity was demonstrated by the antioxidant assays (DPPH and ABTS), underscoring their potential as natural antioxidants. Additionally, the antibacterial tests demonstrated marked inhibitory effects against both *Salmonella enteritidis* and *Escherichia coli* are examples of Gram-negative bacteria. At the same time *Bacillus cereus* and *Staphylococcus aureus* are examples of Gram-positive bacteria. These findings suggest the potential of AgNPs-CmEO as a promising sustainable and cost-effective alternative for biomedical and industrial applications. By leveraging the bioactive properties of *Citrus microcarpa* essential oil, this approach not only promotes green nanotechnology but also expands the functional applications of essential oil-based nanoparticles in diverse fields. Future studies must to concentrate on synthesis optimization parameters and exploring in vivo applications to further validate their efficacy and safety.

ACKNOWLEDGEMENT

The Industrial University of Ho Chi Minh City is deeply appreciated by the authors for giving the support required to conduct this study.

CONFLICT OF INTEREST

The authors declare that they have no conflicts of interest related to this publication.

AUTHOR CONTRIBUTIONS

Each author made a substantial contribution to the work, took part in its review and editing, and gave their approval for the manuscript's release.

FUNDING INFORMATION

No funding was received for this study

REFERENCES

1. Oves M., Aslam M., Rauf M.A., Qayyum S., Qari H.A., *et al.* (2018) Antimicrobial and anticancer activities of silver nanoparticles synthesized from the root hair extract of *Phoenix dactylifera*. *Mater. Sci. Eng. C*, **89**, 429-443.
https://doi.org/10.1016/j.msec.2018.03.035

2. Dhaka A., Mali S.C., Sharma S., and Trivedi R. (2023) A review on biological synthesis of silver nanoparticles and their potential applications. *Results Chem.*, **6**, 101108.
https://doi.org/10.1016/j.rechem.2023.101108

3. Siddiqui M.A., Hasan M., Khan H.A., Rastogi S., and Arora I., Samim M. (2024) Palladium nanoparticles and lung health: Assessing morphology-dependent subacute toxicity in rats and toxicity modulation by naringin. *ACS Omega*, **9**(30), 32745.
https://doi.org/10.1021/acsomega.4c02269

4. Karnwal A., Jassim A.Y., Mohammed A.A., Sharma V., Al-Tawaha A.R.M.S., *et al*. (2024) Nanotechnology for healthcare: Plant-derived nanoparticles in disease treatment and regenerative medicine. *Pharmaceuticals*, **17**(12), 1711.
https://doi.org/10.3390/ph17121711

5. Chen M.H., Yang K.M., Huang T.C., and Wu M.L. (2017) Traditional small-size citrus from Taiwan: Essential oils, bioactive compounds and antioxidant capacity. *Medicines*, **4**(2), 28.
https://doi.org/10.3390/medicines4020028

6. Jena S., Singh R.K., Panigrahi B., Suar M., and Mandal D. (2016) Photo-bioreduction of Ag^{+} ions towards the generation of multifunctional silver nanoparticles. *J. Photochem. Photobiol. B*, **164**, 306-313.
https://doi.org/10.1016/j.jphotobiol.2016.08.048

7. Mohamad N.A.N., Arham N.A., Jai J., and Hadi A. (2014) Plant extract as reducing agent in synthesis of metallic nanoparticles: a review. *Adv. Mater. Res.*, **832**, 350-355.
https://doi.org/10.4028/www.scientific.net/AMR.832.350

8. Kumar S., Basumatary I.B., Sudhani H.P., Bajpai V.K., Chen L., *et al.* (2021) Plant extract mediated silver nanoparticles and their applications as antimicrobials and in sustainable food packaging. *Trends Food Sci. Technol.*, **112**, 651-666.
https://doi.org/10.1016/j.tifs.2021.04.031

9. Maciel M.V.O.B., Almeida A.R., Machado M.H., Elias W.C., Rosa C.G., *et al.* (2020) Green synthesis, characteristics and antimicrobial activity of silver nanoparticles mediated by essential oils. *Biocatal. Agric. Biotechnol.*, **28**, 101746.
https://doi.org/10.1016/j.bcab.2020.101746

10. Qidwai A., Kumar R., and Dikshit A. (2018) Green synthesis of silver nanoparticles by seed of *Phoenix sylvestris* L. and their role in the management of cosmetics embarrassment. Green Chem. *Lett. Rev.*, **11**(2), 176-188.
https://doi.org/10.1080/17518253.2018.1445301

11. Quoc L.P.T. and Phuong L.B.B. (2025) Essential oil from lime peel (*Citrus aurantifolia*) grown in Long an province, Vietnam: Chemical composition and biological activities. *J. Turk. Chem. Soc. Sect. A*, **12**(2), 99-106.
https://doi.org/10.18596/jotcsa.1623631

12. Le H.V.N., Quoc L.P.T., Ho T.H., Raes K., Dam M.S., *et al*. (2023) Green synthesis of silver nanoparticles from extract from *Mentha aquatica* Linn. var. crispa and evaluation of their antibacterial and antioxidant activities. *Herba Pol.*, **69**(1), 37-46.
https://doi.org/10.5604/01.3001.0016.2818

13. Sripahco T., Khruengsai S., Charoensup R., Tovaranonte J., and Pripdeevech P. (2022) Chemical composition, antioxidant, and antimicrobial activity of *Elsholtzia beddomei* CB Clarke ex Hook. f. essential oil. *Sci. Rep*., **12**(1), 2225.
https://doi.org/10.1038/s41598-022-06358-6

14. Basri, D.F. and Sandra, V. (2016) Synergistic interaction of methanol extract from *Canarium odontophyllum* Miq. Leaf in combination with oxacillin against methicillin-resistant *Staphylococcus aureus* (MRSA) ATCC 33591. *Int. J. Microbiol.*, **2016**(1), 5249534.

https://doi.org/10.1155/2016/5249534

15. Ceylan Ö. and Doğru N.H. (2025) Biological activities of silver nanoparticles synthesized using *Olea europaea* L. leaves. *Int. J. Sec. Metab.*, **12**(2), 289-296.
https://doi.org/10.21448/ijsm.1526393

16. Sytu M.R.C. and Camacho D.H. (2018) Green synthesis of silver nanoparticles (AgNPs) from Lenzites betulina and the potential synergistic effect of AgNP and capping biomolecules in enhancing antioxidant activity. *BioNanoScience*, **8**, 835-844.
https://doi.org/10.1007/s12668-018-0548-x

17. Habib T., Caiut J.M.A., and Caillier B. (2022) Synthesis of silver nanoparticles by atmospheric pressure plasma jet. *Nanotechnology*, **33**(32), 325603.
https://doi.org/10.1088/1361-6528/ac6528

18. Wongsa P., Phatikulrungsun P., and Prathumthong S. (2022) FT-IR characteristics, phenolic profiles and inhibitory potential against digestive enzymes of 25 herbal infusions. *Sci. Rep.*, **12**(1), 6631.
https://doi.org/10.1038/s41598-022-10669-z

19. Torrero J., Pérez-Alonso F.J., Peña M.A., Domínguez C., Al-Youbi A.O., *et al.* (2016) In situ infrared study of the electrooxidation of ethanol and acetaldehyde in acid electrolyte. *ChemElectroChem*, **3**(7), 1072-1083.
https://doi.org/10.1002/celc.201600136

20. Mohandas G.G. and Kumaraswamy M. (2018) Antioxidant activities of terpenoids from *Thuidium tamariscellum* (C. Muell.) Bosch. and *Sande-Lac*. a Moss. *Pharmacogn. J.*, **10**(4), 645-649.
https://doi.org/10.5530/pj.2018.4.106

21. Mirzababaei M., Karimiazar J., Teshnizi E.S., Arjmandzadeh R., and Bahmani S.H. (2021) Effect of nano-additives on the strength and durability characteristics of marl. *Minerals*, **11**(10), 1119.
https://doi.org/10.3390/min11101119

22. Kumar B., Smita K., Vizuete K.S., and Cumbal L. (2016) Aqueous phase lavender leaf mediated green synthesis of gold nanoparticles and evaluation of its antioxidant activity. *Biol. Med.*, **8**(3), 1.
https://doi.org/10.4172/0974-8369.1000290

23. Andriotis E.G., Papi R.M., Paraskevopoulou A., and Achilias D.S. (2021) Synthesis of D-limonene loaded polymeric nanoparticles with enhanced antimicrobial properties for potential application in food packaging. *Nanomaterials*, **11**(1), 191.
https://doi.org/10.3390/nano11010191

24. Khan A., Wang C., Sun X., Killpartrick A., and Guo M. (2019) Preparation and characterization of whey protein isolate-DIM nanoparticles. *Int. J. Mol. Sci.*, **20**(16), 3917.
https://doi.org/10.3390/ijms20163917

25. Hussain A., Alajmi M.F., Khan M.A., Pervez S.A., Ahmed F., *et al.* (2019) Biosynthesized silver nanoparticle (AgNP) from *Pandanus odorifer* leaf extract exhibits anti-metastasis and anti-biofilm potentials. *Front. Microbiol.*, **10**, 8.
https://doi.org/10.3389/fmicb.2019.00008

26. Dash S.R., Bag S.S., and Golder A.K. (2018) Synergized AgNPs formation using microwave in a bio-mediated route. *J. Electroanal. Chem.*, **827**, 181-192.
https://doi.org/10.1016/j.jelechem.2018.09.023

27. Saratale R.G., Benelli G., Kumar G., Kim D.S., and Saratale G.D. (2018) Bio-fabrication of silver nanoparticles using the leaf extract of an ancient herbal medicine, dandelion (*Taraxacum officinale*). *Environ. Sci. Pollut. Res.*, **25**(11), 10392-10406.
https://doi.org/10.1007/s11356-017-9581-5

28. Budiarto R., Khalisha A., Sari D.N., Ujilestari T., Wahyono T., *et al*. (2024) Antioxidant properties of lemon essential oils: a meta-analysis of plant parts, extraction methods, dominant compounds, and antioxidant assay categories. *Chem. Biol. Technol. Agric.*, **11**, 147.
https://doi.org/10.1186/s40538-024-00621-w

29. Baroi, A.M., Fierascu, I., Ghizdareanu, A.I., Trica, B., Fistos, T., *et al*. (2024) Green approach for synthesis of silver nanoparticles with antimicrobial and antioxidant properties from grapevine waste extracts. *Int. J. Mol. Sci.*, **25**(8), 4212.
https://doi.org/10.3390/ijms25084212

30. Lestari N.R., Cahyaningrum S.E., Herdyastuti N., Setyarini W., and Arizandy R.Y. (2024) Nanoparticle and binahong (*Anredera cordifolia*) gel modified with Cinnamon essential oil. *Trop. J. Nat. Prod. Res.*, **8**(1), 5936-5945.
http://doi.org/10.26538/tjnpr/v8i1.32

31. Adame M.Y., Shi C., Li C., Aziz T., Alharbi M., *et al*. (2024) Fabrication and characterization of pullulan/tapioca starch-based antibacterial films incorporated with *Litsea cubeba* essential oil for meat preservation. *Int. J. Biol. Macromol.*, **268**, 131775.
https://doi.org/10.1016/j.ijbiomac.2024.131775

32. Song Z., Wu Y., Wang H., and Han H. (2019) Synergistic antibacterial effects of curcumin modified silver nanoparticles through ROS-mediated pathways. *Mater. Sci. Eng. C*, **99**, 255-263.
https://doi.org/10.1016/j.msec.2018.12.053

33. Anuj S.A., Gajera H.P., Hirpara D.G., and Golakiya B.A. (2019) Interruption in membrane permeability of drug-resistant *Staphylococcus aureus* with cationic particles of nanosilver. *Eur. J. Pharm. Sci.*, **127**, 208-216.
https://doi.org/10.1016/j.ejps.2018.11.002